In proc. of the IUTAM Symposium on Dynamics Modeling and Interaction Control in Virtual and Real Environments, 7-11 June, 2010, Budapest, Hungary, IUTAM Book Series by Springer, Vol 30, pp. 11-18., ISBN: 978-94-007-1642-1

The ACROBOTER Platform - Part 2: Servo-Constraints in Computed Torque Control

Ambrus Zelei and Gábor Stépán

Abstract The paper presents the motion control of the ceiling based service robot platform ACROBOTER that contains two main subsystems. The climbing unit is a serial robot, which realizes planar motion in the plane of the ceiling. The swinging unit is hoisted by the climbing unit and it is actuated by windable cables and ducted fans. The two subsystems form a serial and subsequent closed-loop kinematic chain segments. Because of the complexity of the system we use natural (Cartesian) coordinates to describe the configuration of the robot, while a set of algebraic equations represents the geometric constraints. Thus the dynamical model of the system is given in the form of differential-algebraic equations (DAE). The system is under-actuated and the the inverse kinematics and dynamics cannot be solved in closed form. The control task is defined by the servo-constraints which are algebraic equations that have to be considered during the calculation of control forces. In this paper the desired control inputs are determined via the numerical solution of the resulting DAE problem using the Backward Euler discretization method.

1 Introduction

Indoor service robots can effectively use the ceiling of the indoor environment to provide obstacle free motion of the base of these robots, while the carried working units can practically move in the whole inner space of the environment [7]. The present paper describes the motion control of a new service robot platform developed within the ACROBOTER (IST-2006-045530) project [3]. The developed robot

Ambrus Zelei
HAS-BME Research Group on Dynamics of Machines and Vehicles, H-1521 Budapest, Hungary, e-mail: zelei.ambrus@gmail.com

Gábor Stépán
Department of Applied Mechanics, Budapest University of Technology and Economics, H-1521 Budapest, Hungary, e-mail: stepan@mm.bme.hu

utilizing the ceiling for the planar motion, and its cable suspended pendulum-like subsystem is the working unit.

A major challenge in ceiling based locomotion is that the ceiling based unit has to hold the total weight of the robot and the payload safely, and has to provide fast motion of the carried objects at the same time. To satisfy these requirements, permanent magnets are applied to develop a ceiling absorbed mobile base in [7]. In case of ACROBOTER, a serial robot based climbing unit was developed that can crawl on an anchor point system installed on the ceiling (see left in Fig. 1).

The other main subsystem of ACROBOTER is the swinging unit. It is connected to the climbing unit via a windable cable that is called the main cable hereafter. The swinging unit has a mechanical interface to connect different tools. This unit can be positioned and oriented with three orineting secondary cables and ducted fan actuators. For more detailed description of the ACROBOTER design the reader is referred to [3]. The kinematic structure of its planar mechanical model is described in detail in Section 2.

In this paper, first, the dynamical model of the investigated complex robotic structure is described by natural coordinates [2]. The resulting equations of motion are formulated as Lagrangian equations of motion of the first kind. In addition to the introduced geometric constraints, the task of the robot is defined by the so-called servo-constraints which introduce further algebraic equations associated with the original DAE problem of calculating the desired control inputs of the computed torque control (CTC) of ACROBOTER. In the second part of this work the numerical solution of the DAE system of equations is presented by using the Backward Euler discretization method. At the end a real parameter case simulation study is provided to demonstrate the applicability of the proposed controller.

2 Structure of the ACROBOTER platform

The mechanical structure of the ACROBOTER can be seen left in Fig. 1. The climbing unit is an RRT robot that provides the ceiling based locomotion of the system. Its task is to position the suspension point (cable outlet) in the plane of the ceiling. The climbing unit consists of the anchor arm, the rotation arm and a linear axis moving the winding mechanism. The anchor arm swaps between neighboring anchor points, while the rotation arm and the linear axis provide additional two degrees-of-freedom (DoFs). Thus the climbing unit is a kinematically redundant planar manipulator, except in the case when both ends of the anchor arm is fixed to the ceiling. The winding mechanism hoists the swinging unit via the main cable, which unit contains three additional cable actuators. The main role of these cables to control the orientation of the unit, but they also can regulate its elevation yielding a further redundancy. In addition to these cables, three pairs of ducted fans are employed to orient and position the swinging unit. The orienting cables are assumed to be ideal in the model.

In the planar model shown right in Fig. 1, the climbing unit is considered as a single linear axis. The cable connector modeled as a point mass with 2 DoFs and

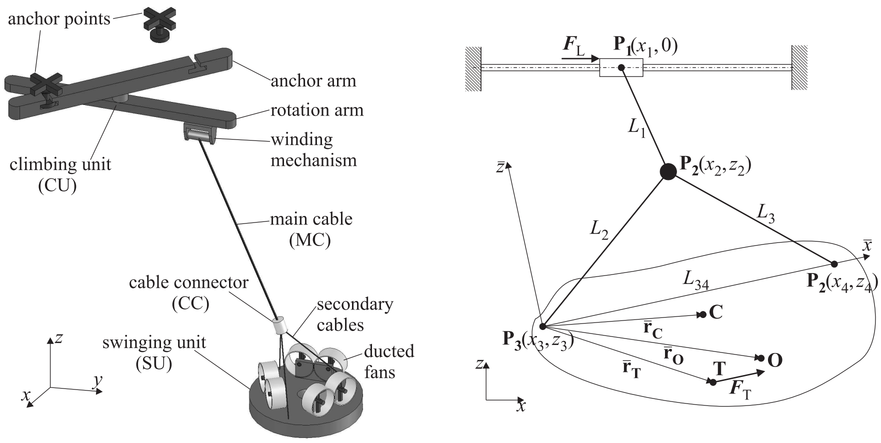

Fig. 1 The ACROBOTER structure (left), planar mechanical model (right)

the swinging unit is a rigid body with 3 DoFs. The kinematics of the swinging unit is described by the redundant set of coordinates associated with points $\mathbf{P}_3$ and $\mathbf{P}_4$.

The total number of DoFs is 6 and we use 7 descriptor coordinates plus one geometric constraint which represents the constant distance L_{34}.

The position of the climbing unit is controlled by the force F_L, while the swinging unit is actuated via the cable forces F_1, F_2 and F_3 and the thrust force F_T. In the model $\mathbf{C}$ denotes the center of gravity of the swinging unit. Point $\mathbf{T}$ determines the line of action of the thrust force F_T being parallel to the local axis $\bar{x}$. And $\mathbf{O}$ is an arbitrarily selected point that has to be controller to move on the desired trajectory.

3 CTC with Backward Euler discretication

The equations of motion (1) and (2) of the system is derived in the form of the Lagrangian equation of motion of the first kind:

$$\mathbf{M}\ddot{\mathbf{q}} + \mathbf{\Phi}_\mathbf{q}^\mathrm{T}(\mathbf{q})\boldsymbol{\lambda} = \mathbf{Q}_g + \mathbf{H}(\mathbf{q})\mathbf{u}\,, \tag{1}$$

$$\boldsymbol{\phi}(\mathbf{q}) = \mathbf{0}\,, \tag{2}$$

where $\mathbf{q} \in \mathbb{R}^n$ denotes the descriptor coordinates and $\mathbf{M} \in \mathbb{R}^{n\times n}$ is the constant mass matrix. In eq. (2) the vector $\boldsymbol{\phi}(\mathbf{q}) \in \mathbb{R}^m$ represents geometric constraints. Matrix $\mathbf{\Phi}_\mathbf{q}(\mathbf{q}) = \partial\boldsymbol{\phi}(\mathbf{q})/\partial\mathbf{q} \in \mathbb{R}^{m\times n}$ is the constraint Jacobian. Vector $\boldsymbol{\lambda} \in \mathbb{R}^m$ contains the Lagrange multipliers and $\mathbf{Q}_g \in \mathbb{R}^n$ is the constant generalized force vector of the gravitational terms. The control input vector is $\mathbf{u} \in \mathbb{R}^l$ is mapped by the input matrix $\mathbf{H}(\mathbf{q}) \in \mathbb{R}^{n\times l}$. The above formalism can directly be applied to the spatial case yielding the same form of the equations of motion as (1) and (2).

The inverse kinematical and dynamical calculations have unique solution if the number of control inputs and the dimension of the task is equal [1]. Thus the task have to be defined by l number of algebraic equations. This set of additional constraint equations are the so-called servo-constraints (control-constraints) $\boldsymbol{\phi}_s(\mathbf{q},\mathbf{p}(t)) = \mathbf{0}$. We assume that these servo-constraint equations can be written in the form $\boldsymbol{\phi}_s(\mathbf{q},\mathbf{p}(t)) = \mathbf{g}(\mathbf{q}) - \mathbf{p}(t)$ where $\mathbf{g}(\mathbf{q})$ represents, for example, the end-effector position of the robot and $\mathbf{p}(t)$ is the performance goal to be realized [1].

For under-actuated robotic systems modeled by Lagrangian equation of motion of the second kind, the computed torque control method was generalized in [6]. The generalized method is called Computed Desired Computed Torque Control (CDCTC) method. Here the expression "computed desired" refers to the fact that a set of uncontrolled coordinates can be separated from the controlled ones, and the desired values of these uncontrolled coordinates have to be calculated by considering the internal dynamics of the system.

The CDCTC method proposed in [6] can be applied to dynamical systems that are described by ordinary differential equations only. This problem can be resolved by projecting the equations of motion 1 and 2 to the subspace of admissible motions associated with the geometric constraints [5]. The simultaneous application of this projection (including the configuration corrections during the numerical solution) and the CDCTC algorithm is complex and computationally expensive. In addition, it has to be noted that the selection of the controlled and uncontrolled coordinates might be highly intuitive in case of complex (non-convetional) robotic structure like ACROBOTER. The introduction of this kind of distinct coordinates is possible only if the servo-constraint equations can be solved in closed form for the set of controlled coordinates.

Instead of the application of the CDCTC method, we apply the Backward Euler discretization for the DAE system the resulting set of implicit equations are solved by the Newton-Raphson method for the desired control inputs $\mathbf{u}$. Considering a PD controller with gain matrices $\mathbf{K}_P$ and $\mathbf{K}_D$ the control law can be formulated as

$$\mathbf{M}\ddot{\mathbf{q}}^d + \boldsymbol{\Phi}_{\mathbf{q}}^{\mathrm{T}}(\mathbf{q}^d)\boldsymbol{\lambda}^d = \mathbf{Q}_g + \mathbf{H}(\mathbf{q}^d)\mathbf{u} - \mathbf{K}_P(\mathbf{q}^d - \mathbf{q}) - \mathbf{K}_D(\dot{\mathbf{q}}^d - \dot{\mathbf{q}}) \,, \tag{3}$$

$$\boldsymbol{\phi}_s(\mathbf{q}^d,\mathbf{p}(t)) = \mathbf{0} \,, \tag{4}$$

$$\boldsymbol{\phi}(\mathbf{q}^d) = \mathbf{0} \,, \tag{5}$$

where superscript d refers to desired quantities. Then, the first order form of equation (3) reads

$$\dot{\mathbf{q}}^d = \mathbf{y}^d \tag{6}$$

$$\dot{\mathbf{y}}^d = \mathbf{M}^{-1}\left[-\boldsymbol{\Phi}_{\mathbf{q}}^{\mathrm{T}}(\mathbf{q}^d)\boldsymbol{\lambda}^d + \mathbf{Q}_g + \mathbf{H}(\mathbf{q}^d)\mathbf{u} - \mathbf{K}_P(\mathbf{q}^d - \mathbf{q}) - \mathbf{K}_D(\dot{\mathbf{q}}^d - \dot{\mathbf{q}})\right] \,. \tag{7}$$

Equations (6) and (7) are first order ordinary differential equations, while equations (4) and (5) are algebraic ones. We use the Backward Euler formula with timestep h to discretize the DAE system, that result in the set of nonlinear algebraic equations for the unknowns desired values $\mathbf{z}_{i+1} = \left[\mathbf{q}^d_{i+1}\ \mathbf{y}^d_{i+1}\ \mathbf{u}_{i+1}\ \boldsymbol{\lambda}^d_{i+1}\right]^{\mathrm{T}}$ in the form:

$$\mathbf{F}(\mathbf{z}_{i+1}) = \begin{bmatrix} \mathbf{q}^d_{i+1} - \mathbf{q}^d_i - h\mathbf{y}^d \\ \mathbf{y}^d_{i+1} - \mathbf{y}^d_i - h\mathbf{M}^{-1}\left[-\boldsymbol{\Phi}^{\mathrm{T}}_{\mathbf{q}}(\mathbf{q}^d_{i+1})\boldsymbol{\lambda}^d_{i+1} + \mathbf{Q}_g + \mathbf{H}(\mathbf{q}^d_{i+1})\mathbf{u}_{i+1} - \mathbf{K}\mathbf{e}\right] \\ \boldsymbol{\phi}_s(\mathbf{q}^d_{i+1}, \mathbf{p}(t_{i+1})) \\ \boldsymbol{\phi}(\mathbf{q}^d_{i+1}) \end{bmatrix} \quad (8)$$

$$\text{with} \quad \mathbf{K} = \left[\mathbf{K}_P \,\vdots\, \mathbf{K}_D\right] \quad \text{and} \quad \mathbf{e} = \begin{bmatrix} \mathbf{q}^d_{i+1} - \mathbf{q}_{i+1} \\ \hdashline \dot{\mathbf{q}}^d_{i+1} - \dot{\mathbf{q}}_{i+1} \end{bmatrix}. \quad (9)$$

For the solution the initial values are $\mathbf{q}^d_0$ and $\mathbf{y}^d_0$ at $i = 0$. They should satisfy the servo-constraints and the geometric constraints. During simulation the initial values of the states $\mathbf{q}_0$ and $\mathbf{y}_0$ only have to satisfy the geometric constraints. The numerical solution of 8 and 9 is based on the well-known Newton-Raphson method. The corresponding Jacobian matrix $\mathbf{J}(\mathbf{z}_{i+1}) = \partial\mathbf{F}(\mathbf{z}_{i+1})/\partial\mathbf{z}_{i+1}$ is calculated numerically, however it could aslo be constructed semi-analytically [4]. Then the iteration

$$\mathbf{z}^{n+1}_{i+1} = \mathbf{z}^n_{i+1} - \mathbf{J}(\mathbf{z}^n_{i+1})\mathbf{F}(\mathbf{z}^n_{i+1}) \quad (10)$$

provides the solution at each time instants, where $\mathbf{z}^n_{i+1}$ is the n^{th} approximation of $\mathbf{z}_{i+1}$. The initial guess $\mathbf{z}^0_{i+1}$ in each time step comes from the best approximation $\mathbf{z}^N_i$ of the previous time step. Usually the Newtor-Raphson iteration converges in $N = 2 \div 6$ steps depending also on the required tolerance.

4 Real parameter case simulation

This section presents the simulation results obtained for the planar model of ACROBOTER shown right in Fig. 1. The selected descriptor coordinates are the Cartesian coordinates of the points $\mathbf{P}_i$, $i = 1\ldots4$ yielding $\mathbf{q} = [x_1\ x_2\ z_2\ x_3\ z_3\ x_4\ z_4]^{\mathrm{T}}$. The control inputs are colleted in vector $\mathbf{u} = [F_L\ F_1\ F_2\ F_3\ F_T]^{\mathrm{T}}$. The single geometric constraint represents the constant distance L_{34} between the points $\mathbf{P}_3$ and $\mathbf{P}_4$ and can be written as:

$$\boldsymbol{\phi}(\mathbf{q}) = \left[(x_3 - x_4)^2 + (z_3 - z_4)^2 - L^2_{34}\right] \quad (11)$$

The mass of the swinging unit is $m_{SU} = 9.3$kg and its moment of inertia with respect to the axis at $\mathbf{P}_3$ is $I_{SU} = 0.4\mathrm{kgm}^2$. The mass of the cable connector is $m_{CC} = 0.5$kg and the mass of the linear drive that represents the climber unit is $m_{CU} = 20$kg. The distance L_{34} is set to be 0.4m. The position of the center of gravity is given by $\bar{\mathbf{r}}_C = [0.2\ 0.05]^{\mathrm{T}}$, while the point of application of the thrust force and the position of point $\mathbf{O}$ are defined by the vectors $\bar{\mathbf{r}}_T = [0.2\ -0.05]^{\mathrm{T}}$ and $\bar{\mathbf{r}}_O = [0.2\ 0]^{\mathrm{T}}$ respectively in the local frame $(\bar{x}, \bar{z})$ measured in meters.

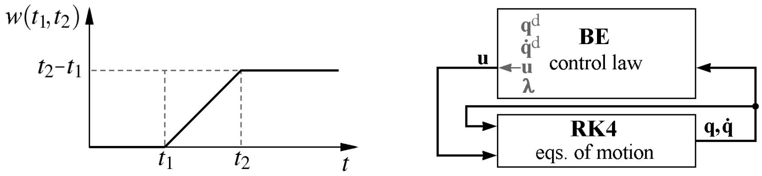

Fig. 2 Modified ramp function (left), block diagram of the simulation (right)

The task of the robot is to track a given trajectory of the point **O**. At the same time the elevation of the cable connector and the horizontality of the swinging unit are also prescribed. The servo-constraint $\boldsymbol{\phi}_s(\mathbf{q},\mathbf{p}(t)) = \mathbf{g}(\mathbf{q}) - \mathbf{p}(t)$ is defined by

$$\mathbf{g}(\mathbf{q}) = \left[x_1 \; z_2 - \frac{z_3+z_4}{2} \; \frac{x_3+x_4}{2} \; \frac{z_3+z_4}{2} \; z_3 - z_4 \right]^{\mathrm{T}} , \tag{12}$$

$$\mathbf{p}(t) = \left[x^d_{CU} \; h^d_{CC} \; x^d_{SU} \; z^d_{SU} \; 0 \right]^{\mathrm{T}} , \tag{13}$$

where the desired climbing unit position $x^d_{CU} = 0.4w(3,4)$, the desired cable connector elevation $h^d_{CC} = 0.8 - 0.2w(2,4)$, the desired swinging unit horizontal position $x^d_{SU} = 0.2w(2,4)$ and the vertical position $z^d_{SU} = -1.5 + 0.4w(2,4)$ are given in meters and they are used to calculate the reference values of the controller. The corresponding weighting functions $w(2,4)$ and $w(3,4)$ are defined by $w(t_1,t_2)$ as shown in Fig. 2. In the investigated simple case, it is possible to solve the servo-constraint equations and the geometric constraint equation for the intuitively chosen set of controlled coordinates $\mathbf{q}_c = [x_1 \; z_2 \; x_3 \; z_3 \; z_4]^{\mathrm{T}}$. with $\mathbf{q}_u = [x_2 \; x_4]^{\mathrm{T}}$. The corresponding solution for the controlled coordinates reads:

$$x_1 = x^d_{CU}, \;\; z_2 = z^d_{SU} + h^d_{CC}, \;\; x_3 = x^d_{SU} - \frac{L_{34}}{2}, \;\; z_3 = z^d_{SU} \text{ and } z_4 = z^d_{SU} \tag{14}$$

The uncontrolled coordinate x_4 comes directly from the geometric constraint equation. Despite of the available closed form solution, here, we do not separate the controlled and the uncontrolled coordinates. Instead the servo-constrains are directly attached to the control law (3-5) proposed in Section 3.

The equations of motion was solved using the fourth order Runge-Kutta method, and the control input was calculated by the simultaneously applied Backward-Euler algorithm as shown in Fig. 2. The simulation of the DAE system was accomplished by using Baumgarte's method [2] under the assumption that the geometric constraints do not depend on time explicitly:

$$\begin{bmatrix} \mathbf{M} & \boldsymbol{\Phi}^{\mathrm{T}}_{\mathbf{q}} \\ \boldsymbol{\Phi}_{\mathbf{q}} & \mathbf{0} \end{bmatrix} \begin{bmatrix} \ddot{\mathbf{q}} \\ \boldsymbol{\lambda} \end{bmatrix} = \begin{bmatrix} \mathbf{Q}_{\mathbf{g}} + \mathbf{H}\mathbf{u} \\ -\dot{\boldsymbol{\Phi}}_{\mathbf{q}}\dot{\mathbf{q}} - 2\alpha\boldsymbol{\Phi}_{\mathbf{q}}\dot{\mathbf{q}} - \beta^2\boldsymbol{\phi} \end{bmatrix} \tag{15}$$

In equation (15) $\alpha = 40$ and $\beta = 60$ are constant numbers that effects the suppression of the geometric constraint errors. The time step of the simulation was set to $h = 0.01\mathrm{s}$.

Using the experimentally tuned gain matrices $\mathbf{K}_P = \mathrm{diag}(150, 0, 10, 1, 3, 1, 3)$ and $\mathbf{K}_D = \mathrm{diag}(1000, 0.5, 10, 15, 20, 15, 20)$, the simulated motion of the system is presented in Fig. 3, where panel (a) shows the stroboscopic motion of the planar ACROBOTER. The realized path of point **O** is denoted by the thick curve that slightly oscillates around, but converges to the desired path depicted as a thin straight line. The desired configurations are shown by dashed lines, while the continuous lines presents the realized configurations of the robot. According to the task equations (12) and (13) the robot is commanded to stand still till $t = 2$s, then the reference point **O** is commanded to move along a straight line with constant velocity. During the same period of time the desired elevation of the cable connector is decreasing.

The climbing unit is commanded to start moving with constant velocity at $t = 3$s. Then, at $t = 4$s the task is to keep the swinging unit in a certain fixed position. Panel (b) in Fig. 3 shows the constraint violation with the maximum of 4mm. Note that the constraint violation depend on the α and β parameters of eq. (15). Panels (c) and (d) show the servo-constraint errors. The error in the climbing unit's position is $\phi_{s,1}$, the elevation error of the cable connector is $\phi_{s,2}$, the horizontal and vertical position errors corresponding to the coordinates of point **O** are $\phi_{s,3}$ and $\phi_{s,4}$ and the orientation error of the swinging unit is $\phi_{s,5}$ (see eqs. (12) and (13)).

The servo-constraint errors show that the large initial errors decreasing in the first 2 second. Then the sudden change of the desired velocities causes further, but settling oscillations. When the system has to stop at $t = 4$s the oscillations are suppressed, too. However, the relatively high frequency oscillation of $\phi_{s,4}$ dies out slowly. This corresponds to the oscillations of the cable connector having relatively

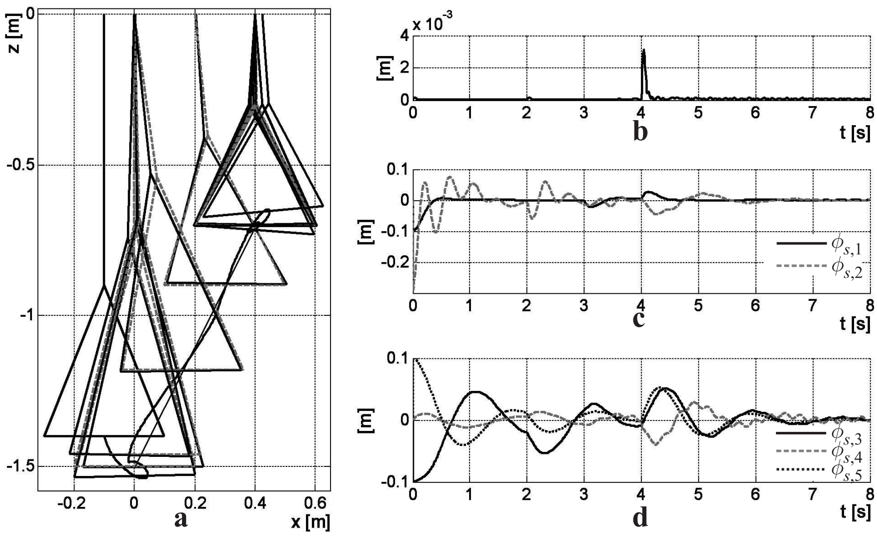

Fig. 3 Simulation results: (a) stroboscopic movement of the system, (b) violation of the geometric constraint, (c) and (d) servo constraint violations

small mass compared to the swinging unit. It is hard to suppress the horizontal vibration of the cable connector due to the under-actuated character of the robot. These oscillations could be decreased by prescribing smooth trajectories.

5 Conclusions

The computed torque control method was generalized and applied for the tracking control of ACROBOTER using descriptor type system modeling. In contrast to [6], the control inputs were determined via the direct solution of the corresponding DAE problem. The control task was defined by servo-constraint equations incorporated in the algebraic equations. Considering the experimentally tuned control parameters the presented simulation results show the applicability of the proposed simple PD controller for the tracking control of the under-actuated ACROBOTER system.

Acknowledgements This work was supported in part by the Hungarian National Science Foundation under grant no. OTKA K068910, the ACROBOTER (IST-2006-045530) project and the HAS-BME Research Group on Dynamics of Machines and Vehicles.

References

[1] Blajer W, Kolodziejczyk K (2008) Modeling of underactuated mechanical systems in partly specified motion. Journal of Theoretical and Applied Mechanics 46(2):383–394
[2] de Jalón JG, Bayo E (1994) Kinematic and dynamic simulation of multibody systems: the real-time challenge. Springer-Verlag
[3] Kovács LL, Zelei A, Bencsik L, Stépán G (2010) Conceptual design and dynamics modeling aspects of acroboter. In: Proceedings of the IUTAM Symposium on Dynamics Modeling and Interaction Control in Virtual and Real Environments, Budapest, pp xxx–yyy
[4] Kovács LL, Zelei A, Bencsik L, Turi J, Stépán G (2010) Motion control of an under-actuated service robot using natural coordinates. In: RoManSy 18 - Robot Design, Dynamics and Control, Udine, Italy, pp 331–338
[5] Kövecses J, J-C Piedoboeuf CL (2003) Dynamic modeling and simulation of constrained robotic systems. IEEE/ASME Transactions on mechatronics 8(2):165–177
[6] Lammerts IMM (1993) Adaptive computed reference computed torque control. PhD thesis, Eindhoven University of Technology
[7] Sato T, Fukui R, Mofushita H, Mori T (2004) Construction of ceiling adsorbed mobile robots platform utilizing permanent magnet inductive traction method. In: Proceedings of 2004 IEEEiRSJ International Conference on Intelligent Robots and Systems, pp 552–558